



(RESEARCH ARTICLE)



Derived Functions for MATLAB Non-Linear Solvers: An optimal rotor slot and bar design stopgap

Nelson Oyakhilomen Omogbai *

Department of Electrical Engineering, Nnamdi Azikiwe University, Awka, Anambra State, Nigeria.

World Journal of Advanced Engineering Technology and Sciences, 2023, 08(01), 382–390

Publication history: Received on 13 January 2023; revised on 21 February 2023; accepted on 23 February 2023

Article DOI: <https://doi.org/10.30574/wjaets.2023.8.1.0060>

Abstract

The most striking difference between the Squirrel cage induction motor (SCIM) and other electric motors lies invariably in the rotor. The major running performance characteristics, together with the entire acceleration performance range, are all influenced, in varying degrees, by the rotor slot and bar design. Therefore, proper dimensioning of the slots and bars is therefore critical to attaining a high performing machine. The preliminary stage of the SCIM design, if well done, facilitates the refinement and optimization stages; serving as a good take-off point for ultimately realizing that final state of the art design. This study therefore attempts to derive relevant design functions that could be fed into the algorithms of various non-linear solvers, one of which is the Genetic Algorithm (GA), to output the rotor slot initial main dimensions for the SCIM; from where proper design refinement/optimization could cheaply evolve. The SCIM design obtained from implementing the derived equations, when compared with the appropriate reference datasheets, showed only minor deviations from the expected performance indices – an outcome deemed satisfactory for a preliminary design attempt. The so obtained initial dimensions may in practice be subjected to the appropriate refinement, depending on the target performance requirement of the motor to be designed.

Keywords: Objective function; Constraint function; Rotor slot design; Genetic Algorithm; MATLAB; Non-linear solvers.

1. Introduction

Most of the induction motors employed in the industry have squirrel cage rotor due to its simple and robust construction. The Squirrel cage induction motor (SCIM) rotor consists of a laminated cylindrical core having slots at the outer periphery. Copper or aluminum bar conductors are placed in these slots and short circuited at each end by copper or aluminum rings. Thus, the rotor winding is permanently short-circuited and no external resistance can be added in the rotor circuit. The slots are skewed compared to the shaft to obtain smooth and sufficient torque, reduce the magnetic locking of the stator and rotor, and to increase the rotor resistance since the length of the rotor bar conductor is increased.[1],[2].

The induction motor design is considered a nonlinear programming problem, where one or more objective cost functions of the design are minimized. One of the most important parameters in the design of electric motors is the determination of stator and rotor slot geometries. The use of different slot geometries in motors significantly changes the motor performance via the variation of equivalent circuit parameters. For this reason, it is of great importance that the slot geometries are properly selected when designing the motor [13].

The geometric configuration of the rotor slot and bar cross section, combined with bar material conductivity, virtually controls the balance of several significant performance characteristics of medium and large induction motors [4]. Substantial improvements from previous studies have shown that the rotor slot geometry design plays a critical role in

* Corresponding author: Omogbai Nelson Oyakhilomen

improving the motor performance, because torque speed characteristics are largely determined by the rotor configurations [7], [8]. Among the several design factors affecting the SCIM performance, the shape of the slot hosting the rotor bars, plays a fundamental role in defining the torque-speed curve as well as the efficiency as a function of the load [5].

There is no unique solution to a design problem, and designs for the same specification will differ because of different emphasis being placed on each requirement by the particular designer [11]. In order to eliminate the few drawbacks of the SCIM, the designer usually makes a preliminary modeling and determines the physical size via parametric optimization with modern software in accordance with the requirements of the application. [12]. Usually, the rotor slot geometry can be considered as an independent design parameter [10]. Rotor slot design has traditionally been a process of evolution; the designer begins with an existing slot shape and alters the dimensions in a cut-and-try approach until the performance specification is met. Alternatively, a formal method is employed, in which the slot dimensions are altered deterministically until the desired performance is achieved [9].

References [3, 6, 16 - 20] are some recent and readily available articles that have accomplished objectives that are similar to that of this present treatise, making use of CAD tools like the Mat Lab, MagNet, Visual Basic, Artificial Neural Networks, finite element etc. However, none of them actually went on to derive relevant customizable functions that are executable by MATLAB nonlinear solvers. In this paper, some pertinent equations specially tailored to the rotor slot and bar geometry were derived from the design experience of various authors, and suitably formatted for compatibility with common nonlinear optimization tools or solvers that are usually employed in SCIM design. The nonlinear solver to be illustratively employed is the MATLAB based Genetic Algorithm (GA). The GA is a potent tool for carrying out the design/optimization of electrical machinery. One of the merits of the GA is that it is useful for solving nonlinear equations or complex optimization problems where the number of parameters is large, and it finds the global minimum for a wide range of functions, instead of a local minimum, without the need for the starting points to be close to the actual values [14]. Another advantage is that it does not require the use of the derivative of the function, which is not always easily obtainable or may not even exist [15],

This work hopes to serve as a valuable piece of reference in various modules of SCIM design classes in tertiary institutions, and for the design engineer in practice; the results obtained from implementation promises to be a rough and ready take off point for the optimization of the rotor slot geometry. The author has attempted to treat the stator version in [25].

2. Material and methods

In fulfilling the aim of this study, various electromechanical equations or expressions directly or indirectly pertaining to the SCIM rotor slot dimensioning were identified from seasoned machine design literature, and mathematically formatted to be machine readable/executable by the GA routine in MATLAB, as well as by other solvers/techniques that are syntactically akin to the GA. It is important to highlight that this paper experiments with a standard efficiency 75HP three-phase induction motor with symmetric windings and squirrel cage rotor.

It is assumed that the SCIM main dimensions and other design variables of the stator as well as the rotor have been fully designed for the given rating, and are all functionally integrable to any compatible rotor slot design, including that hereinafter outlined. The geometry of the rotor slot is shown in fig 1 with the rotor bar indicated by the shaded portion.

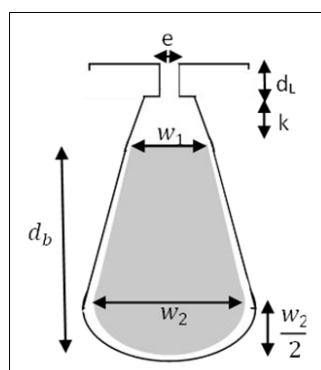


Figure 1 Rotor slot geometry

Table 1 Test Machine specifications

Specifications of Test Machine	Values
Power rating (HP)	75
Voltage L-L (V) volts	400
Number of poles (p)	6
Number of rotor slots (Sr)	55
Number of stator slots (Ss)	72
Flux per pole (phi) wb	0.022168468
Bore diameter (D) mm	370.9480152
Stator core outer diameter (Do) mm	561.1678999
Core axial length (L) mm	194.2279266
Airgap length (lg) mm	0.970623175
Stator coil leakage reactance X1 (ohms)	0.109421793
Magnetizing reactance Xm (ohms)	4.741771839
Stator coil resistance R1 (ohms)	0.055371997
Core loss resistance Rc (ohms)	157.5086264

For simplicity, all slots and slot components were assumed to be in the form of simple geometric shapes, and the laws of geometry and trigonometry were thus assumed to apply accordingly. The GA was called to derive the main rotor slot parameters such that both the rotor teeth and the core may not attain unacceptable levels of magnetic saturation.

The following outlines the general Matlab syntax by which GA finds the minimum of a function.

$$[x,fval] = ga(\text{fitnessfcn},nvars,A,b,Aeq,beq,LB,UB,\text{nonlcon},\text{options})\dots\dots\dots(1)$$

Where,

‘x’ is the best point that GA located during its iterations.

‘fval’ is the fitness function evaluated at x.

‘fitnessfcn’ is the handle to the fitness function.

‘nvars’ is the positive integer representing the number of variables in the problem.

‘A’ & ‘b’ is the matrix & vector respectively, for the linear inequality constraints of the form

$$A*x \leq b \dots\dots\dots(2)$$

‘Aeq’ & ‘beq’ is the matrix & vector respectively, for the linear equality constraints of the form

$$Aeq*x = beq \dots\dots\dots(3)$$

‘LB’ & ‘UB’ are the vectors of lower & upper bounds respectively.

'nonlcon' is the nonlinear constraint function handle that returns two outputs:

$$[c,ceq] = \text{nonlcon}(x) \quad \dots\dots\dots(4)$$

'options' is the structure containing optimization options.

2.1. Deriving the objective function

Equation 5 culled from [21] was used to derive the *fitnessfcn* of equation 1, with relevant adjustment made to suit the rotor geometry.

$$\text{Rotor minimum tooth width } w_{rt} (\text{min}) = \frac{p\phi}{B_{r_{\max}}LS_rS_r} \quad \dots\dots\dots(5)$$

L is the core axial length, S_r is the number of rotor slots, φ is the air gap flux per pole, number of poles is given as p, S_r represents the rotor core stacking factor, while B_{r_{max}} is the maximum tooth flux density corresponding to the rotor tooth width w_{rt}.

From fig 1 and equation 5:

$$K_1/w_{rt} \leq B_r \quad \dots\dots\dots(6)$$

Where, by modifying for the peak value

$$K_1 = \frac{\pi p\phi}{LS_rS_r} \quad \dots\dots\dots(7)$$

The rotor slot pitch λ_r used was that at the extreme closest to the rotor shaft, since tooth saturation appears most probable at that region for this shape of rotor slot/bar. Thus,

$$w_{rt} \approx \lambda_r - w_2 \quad \dots\dots\dots(8)$$

$$w_{rt} \approx \frac{\pi(D_r - 2d_L - 2d_b - 2k + w_2)}{S_r} - w_2 \quad \dots\dots\dots (9)$$

$$\approx k_2(k_3 - 2d_b + w_2) - w_2 \quad \dots\dots\dots (10)$$

Where, D_r is the rotor diameter and

$$k_3 = D_r - 2d_L - 2k \quad \dots\dots\dots (11)$$

while,

$$k_2 \approx \frac{\pi}{S_r} \quad \dots\dots\dots (12)$$

Therefore, the fitness function (ObjFcn or fitnessfcn) from equation 6 is:

$$K_1 - B_r w_{rt} \leq 0 \quad \dots\dots\dots(13)$$

Which on substituting equation 10 expands to:

$$K_1 + 2B_r d_b k_2 + B_r w_2 - B_r k_2 k_3 - B_r k_2 w_2 \leq 0 \quad \dots\dots\dots(14)$$

2.2. Deriving the constraints function

References [11, 22] also gave the approximate relationship between the tooth flux density B and the airgap average flux density B_{av} over one slot pitch for the case where saturation is neglected i.e.

$$\lambda B_{av}/w_{rt} \leq B \quad \dots\dots\dots(15)$$

This ideal case was used with relevant adjustments, as the nonlinear constraint (nonlcon) to guide the GA towards a suitable solution. Where, by modifying for the peak value;

$$B_{av} \approx \frac{\frac{\pi}{2} p \phi}{\pi L S_f D_{rt}} = \frac{k_4}{D_{rt}} = \frac{k_4}{k_3 - 2d_b + w_2} \quad \dots\dots\dots(16)$$

$$\text{Where, } k_4 = \frac{\frac{\pi}{2} p \phi}{\pi L S_f} \quad \dots\dots\dots(17)$$

$$D_{rt} \approx k_3 - 2d_b + w_2 \dots\dots\dots(18)$$

Recall from equation 8 and 9 that,

$$\lambda_r \approx k_2(k_3 - 2d_b + w_2) \quad \dots\dots\dots(19)$$

$$\text{Then, equation 15 becomes: } \frac{k_4}{k_3 - 2d_b + w_2} \cdot \frac{k_2(k_3 - 2d_b + w_2)}{k_2(k_3 - 2d_b + w_2) - w_2} \leq B_r \quad \dots\dots\dots(20)$$

On simplifying equation 20, the nonlinear constraint *nonlcon* is therefore:

$$k_2 k_4 - B_r(k_2 k_3 - 2k_2 d_b + k_2 w_2 - w_2) \leq 0 \quad \dots\dots\dots(21)$$

But from [23];

$$w_2 \approx w_1 + 2(d_b - \frac{w_2}{2}) \text{ tank}_2 \quad \dots\dots\dots(22)$$

$$\text{Since } \text{tank}_2 \approx k_2, \text{ then: } w_2 \approx w_1 + 2(d_b - \frac{w_2}{2}) k_2 \dots\dots\dots (23)$$

The linear inequality constraint function for equation 2 may therefore take the form:

$$w_2 + k_2 w_2 - 2d_b k_2 > 0 \quad \dots\dots\dots (24)$$

Having got the values for the unknown slot variables from the GA output, w_1 could be computed from equation 22

$$\text{thus: } w_1 \approx w_2 - 2(d_b - \frac{w_2}{2}) \text{ tank}_2 \quad \dots\dots\dots (25)$$

2.3. Deriving the function for the bounds

Reference [21] also gave the expression for the minimum and maximum depth of rotor core

$$d_c(\text{min/max}) = \frac{\phi}{2 B_{rc(\text{max/min})} L S_f} \dots\dots\dots(26)$$

The upper bounds (UB) values for the variables, are usually the critical bounds: therefore $d_{b\text{max}}$ was got from equation 26 by substituting the geometric equivalent of d_c from fig 1 and taking ϕ as the peak flux per pole: Taking the maximum limit of the rotor core flux density $B_{rc(\text{max})}$ as $2T$ and under the assumption that no flux passes through the shaft of diameter D_{sh} , then $d_{b\text{max}}$ can be shown to be:

$$d_{b\text{max}} = \frac{B_{rc\text{max}}(D_r - (D_{sh} + 2d_v + 2d_L + 2k)) - (\frac{\phi}{L S_f})}{2 B_{rc\text{max}}} \quad \dots\dots\dots(27)$$

d_v being the air duct diameter

$$\text{The limit for } w_2 \text{ as derived from equation 9 gives: } w_{2\text{max}} \approx \frac{S_r w_{rt} - \pi(D_r - 2d_L - 2k)}{\pi - S_r} \quad \dots\dots\dots(28)$$

For this rotor bar that tapers from the rotor shaft towards the gap, it was assumed that the rotor tooth width w_{rt} is less than 50% of the slot pitch λ_r at the shaft end, Therefore, the upper limit of w_{rt} was fixed at $0.5\lambda_r$, and hence equation 28 becomes:

$$w_{2max} \approx \frac{0.5S_r\lambda_r - \pi(D_r - 2d_L - 2k)}{\pi - S_r} \dots\dots\dots(29)$$

With the above equations, the GA outputs three variables (nvars = 3) i.e B_r , d_b and w_2 .

2.4. Other related dimensions

The area of the rotor bar section A_b , approximated to a composite shape comprising a semicircle and a trapezium, was then computed as:

$$A_b \approx 0.125\pi w_2^2 + 0.5d_h(w_1 + w_2) \dots\dots\dots(30)$$

d_h being the height of the trapezoidal portion of the bar bounded by w_1 and w_2 .

Reference [24] opines that the CSA of the endring (taken as rectangular), carrying a current I_e of density d_{en} , could be taken as:

$$A_{er} = I_e/d_{en} \dots\dots\dots(31)$$

Therefore, the width (of A_{er}),

$$w_{er} = A_{er}/d_{er} \dots\dots\dots(32)$$

The endring depth d_{er} may be taken equal to the bar depth for simplicity.

The endring mean diameter

$$D_{er} = D_r - (d_{er} + 2d_L) \dots\dots\dots(33)$$

Equations 14, 21, 24, 27 through 30 are the proposed formatted design functions for driving the GA or any syntactically similar optimization tool/solver, to obtain the rotor slot initial main sizing parameters prior to any further refinement or optimization procedures.

3. Results and discussion

Table 1 gives the specification of the test machine whose performance is compared with that of the standard efficiency class of SCIM's as archived by seasoned international industrial leaders involved in the commercial production of electrical machinery in compliance with the IEC guidelines. The GA outputted main rotor slot dimensions are given in table 2.

Table 2 GA output

GA output and related parameters	Values
Bar width at the top (w_1) mm	7.278709099
Bar width at the bottom (w_2) mm	8.977074556
Bar depth (d_b) approx. endring depth (d_{er}) mm	18.5849273
Rotor tooth width @ max. Brt (w_{rt}) mm	9.743424894
CSA of rotor bar (A_b) sq mm	146.2207148
CSA of endring (A_{er}) sq mm	387.8624925

Rotor slot opening (e) mm	4.852472733
Rotor tooth lip depth (dl) mm	3.28512404
Clearance of rotor bar from slot opening (k) mm	3.2512
Maximum Rotor tooth flux density (Brt) T	2.089918523

It is necessary to compare the performance of the SCIM realized from implementing the rotor slot derived functions, with those of salable prototypes in relevant catalogues; so as to ascertain how close to real life the test machine is, and thus, ascertain the suitability of the derived functions as reliable providers of pre-refined dimensions for the rotor slot; when the said functions are run in compatible Matlab solvers. This comparison was done in table 3.

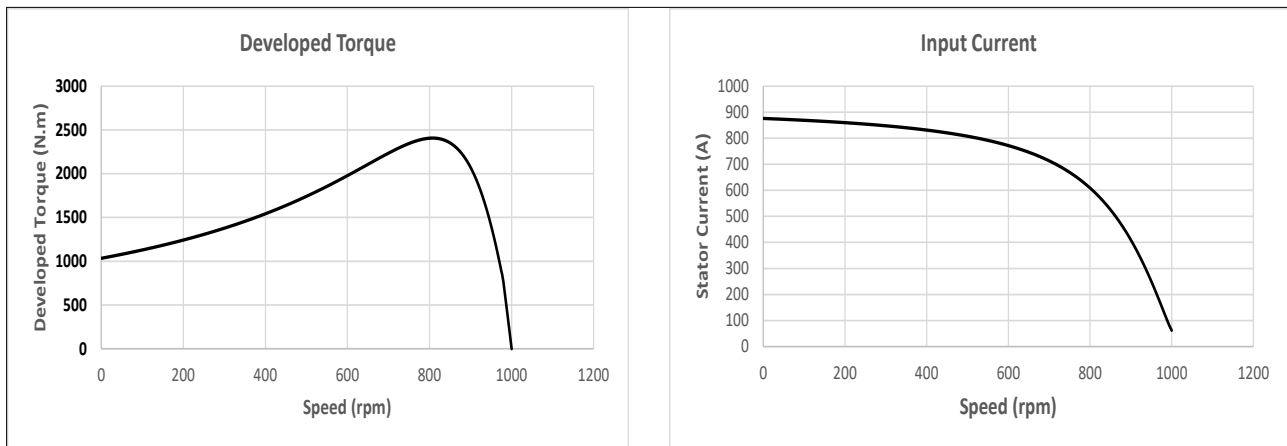


Figure 2 Characteristic curves of Test Machine

It may be observed that, despite the fact that the test machine houses a rough and ready rotor slot design, its characteristic curves of fig 2 follows the expected trend for a typical SCIM of the given rating; and from table 3, it does appear to perform impressively in the area of power factor and capacity for short time overload (as the Maximum to Full load torque ratio tends to indicate). The design also seems good in the area of low slip operation (as most of the full load data indicate). However, minor deviations are most obvious in the ratios – as seen in Starting to Full load torque ratio. Also, its full load efficiency and its suitability for direct on line starting (as seen in the starting to full load current ratio) does not look quite impressive. Overall, the performances of the test machine appear adequate for the machine rotor slot dimensions as well as the derived functions, to be adopted as a good takeoff point to facilitate subsequent design refinement/optimization, depending on target performance or application.

Table 3 Comparison of SCIM performance with that of standard prototypes

Parameters	ABB Motors (M2QA Series)	Vemat Motors (3VTB Series)	WEG Motors (W22 Series)	OMEC Motors (OMT1 Series)	Test Machine
Full Load Efficiency	0.92	0.94	0.93	0.92	0.91
Full Load Power Factor	0.88	0.82	0.81	0.83	0.85
Full Load Current (AMPS)	98	103	106	104	104
Full Load Speed (RPM)	985	992	985	985	988
Starting to Full load current ratio	7	6.8	6	7	8.4
Starting to Full load torque ratio	2.3	2.3	2.2	2.1	1.9
Maximum to Full load torque ratio	2.5	2.6	2.5	2.3	4.4

4. Conclusion

With the primary objective of providing handy equations/functions for realizing good starting values in the rotor slot dimension search space for various 3ph SCIM optimization programs, relevant design functions have been derived and formatted for driving nonlinear solvers or optimization tools such as the GA and the likes, as far as the preliminary rotor slot dimensioning in a typical SCIM design program is concerned; and the algorithm has been integrated into an existing SCIM program in Matlab for proper overall machine performance assessment. The machine performance has been assessed against frontline industrial prototypes. The results obtained show that though the rotor dimensions, in particular, are yet in their unrefined state, the test machine in which they feature, could arguably pass for a final salable prototype. Therefore, designers, students, and researchers are in [25] and herein provided with handy equations and formatted functions to possibly kickstart and facilitate their design and optimization routines, with relevant modifications possible where necessary; to capture the peculiarities of other rotor (and/or stator) slot geometries.

Compliance with ethical standards

Acknowledgments

Due appreciation goes to the following impactful personalities who in the following ways and more, have been of immense assistance: Professor E. U. Ubeku, of the Electrical Engineering department of the University of Benin and Professors O. A. Ezechukwu and E. A. Anazia of the Electrical Engineering department of the Nnamdi Azikiwe University, for their unassuming support. MathWorks and Microsoft conglomerates for putting together very effective virtual laboratory environments. Mr. Festus Odijie, Dr. Courage Omogbai, Mrs. Veronica Omogbai for their much-valued mentorship.

Disclosure of conflict of interest

The author declares that no competing interests exist.

References

- [1] Sahdev, SK. (2018). *Electrical Machines*. Cambridge: Cambridge University Press.
- [2] Senty, S. (2012). *Motor Control Fundamentals*. Clifton Park, N.Y: Delmar.
- [3] Boglietti A. Cavagnino A. Lazzari M. Vaschetto S. (2012). Preliminary induction motor electromagnetic sizing based on a geometrical approach. *IET Electr. Power Appl.* Vol. 6(9) pp. 583–592 583 doi: 10.1049/iet-epa.2012.0037.
- [4] Boglietti, A. Cavagnino, A. and Lazzari, M. (2007) “Geometrical approach to induction motor design,” in *Conf. Rec. IEEE-IECON, Taipei, Taiwan, Nov. 5–8, 2007*, pp. 149– 156.
- [5] Di Nardo, M., Marfoli, A., Degano, M., and Gerada, C. (2021). Open and Closed Rotor Slots Design of Single and Double Cages Induction Motor. *IEEE Workshop on Electrical Machines Design, Control and Diagnosis (WEMDCD)*. DOI: 10.1109/WEMDCD51469.2021.9425665.
- [6] Zhang, D. Park, CS. and Koh, CS. (2011). A new optimal design method of rotor slot of three- phase squirrel cage induction motor for NEMA class D speed-torque characteristic using multi- objective optimization algorithm. *IEEE Transactions on Magnetics*. 48 (2), 879 – 882. Doi: 10.1109/TMAG.2011.2174040.
- [7] Lee, GS. Min and Hong, JP. (2013). Optimal Shape Design of Rotor Slot in Squirrel-Cage Induction Motor Considering Torque Characteristics. *IEEE Transactions on Magnetics*. vol. 49(5), pp. 2197–2200. ISSN 1941-0069. DOI: 10.1109/TMAG.2013.2239626.
- [8] Zhang, K., Jiang, X., Wu, Y., Zhang, L. and Wu, X. (2010). Effect of slot shape in rotor of electrical motor with high-speed spindle on slot ripples. In: *Proceedings of the 2010 International Conference on Modelling, Identification and Control*. Okayama: IEEE, 2010, pp. 670–675. ISBN 978-0- 9555293-3-7.
- [9] Williamson, S, & McClay, CJ. (1996). Optimization of the Geometry of Closed Rotor Slots for Cage Induction Motors. *IEEE Transactions on Industry Applications*, Vol. 32(3).

- [10] Galindo, VA., Lopez-fdez, XM., Pinto, JAD. and Coimbra, AP. (2002). Parametric Study of Rotor Slot Shape on a Cage Induction Motor. *Studies on Applied Electromagnetics and Mechanics*. 190 – 195. Vol 22.
- [11] Lipo TA. (2017). *Introduction to AC Machine Design*. New Jersey: IEEE Press, John Wiley & Sons, Inc. PP. 251 – 302.
- [12] Tezcan MM Yetgin GA Canakoglu AI Cevher B Turan M and Ayaz M. (2018). Investigation of the effects of the equivalent circuit parameters on induction motor torque using three different equivalent circuit models. *MATEC Web of Conferences* 157, 01019. <https://doi.org/10.1051/mateconf/201815701019>.
- [13] Yetgin AG and Durmus B. (2021). Optimization of slot permeance coefficient with average differential evolution algorithm for maximum torque values by minimizing reactances in induction machines. *Ain Shams Engineering Journal*. <https://doi.org/10.1016/j.asej.2021.01.012>.
- [14] Raghuram A. Shashikala V. (2013). Design and Optimization of Three Phase Induction Motor using Genetic Algorithm. *International Journal of Advances in Computer Science and Technology*, Vol. 2(6), pp. 70 – 76.
- [15] Çunkas M. and Akkaya R. (2006). Design Optimization of Induction Motor by Genetic Algorithm and Comparison with Existing Motor. *Mathematical and Computational Applications*, Vol. 11(3), pp. 193-203, Association for Scientific Research.
- [16] Alteheld C. and Gottkehas Kamp R. (2019). Automated Preliminary Design of Induction Machines Aided by Artificial Neural Networks. 2019 International Conference on Electrical Drives & Power Electronics (EDPE). IEEE.
- [17] Bitsi K. Wallmark O. Beniakar ME. and Bosga SG. (2020). Preliminary Electromagnetic Sizing of Axial-Flux Induction Machines. *IEEE ICEM*.
- [18] Aguiar VPB, Neto TRF and Ricardo STP. (2016). Three-Phase Induction Motor Preliminary Design assisted by CAD Software based on Brazilian Standards.
- [19] Sadagopan SM. (2015). Design of Outer Rotor Induction Motor Alternative to PMSM With Fixed Stator. A Master thesis submitted to McGill University. Swathi Meenakshi Sadagopan,
- [20] Somashekar B. (2015). Design of three Phase Induction Motor using Mat Lab Programming. *International Journal on Recent and Innovation Trends in Computing and Communication* Volume: 3 (8). <http://www.ijritcc.org>.
- [21] Toliyat HA. and Kliman GB. (2004). *Handbook of Electric Motors*. Florida: Taylor & Francis Group. PP. 263 – 265.
- [22] Sawhney AK. (2009). *A Course in Electrical Machine Design*, Dhanpat Rai Publication, India.
- [23] Boldea, I. and Nasar, SA. (2010). *The Induction Machine Handbook*. Washington, D.C: CRC Press, Taylor & Francis Group. PP. 447 – 473.
- [24] Cathey, JJ. (2001). *Electric machines: analysis and design applying Matlab*. New York: McGraw-Hill Higher Education. PP. 317 - 420.
- [25] Omogbai, ON. (2023). Derived Functions for MATLAB Non-linear Solvers – an optimal Stator Slot Design Stopgap. *Journal of Engineering Research and Reports*. Volume 24(4), Pp. 8-14. DOI: 10.9734/JERR/2023/v24i4809